Isothermal Growth of Hydrogen Bubbles During Electrolysis

D. E. WESTERHEIDE and J. W. WESTWATER

University of Illinois, Urbana, Illinois

The investigation was concerned with measuring growth rates of bubbles in an isothermal medium where growth is controlled by mass diffusion. The conditions were met by generating hydrogen bubbles at a platinum cathode during the electrolysis of water. Growth data were obtained by motion picture photography at 800 to 2,400 frames/sec. taken through a microscope to produce an enlargement of 30X on the film.

Growth took place in 0.1 normal and 1.0 normal sulfuric acid in water at 77°F. Current densities between 0.1 and 0.2 amp./sq. cm. were used. The observed diameters were all less than 0.006 in., and the growth times were less than 2 sec. Beside growth phenomena interesting features recorded included the coalescence of bubbles, the jumping of bubbles off the solid and then back again, and the slip of the bubble contact at the solid surface.

Some bubbles grew with their radii proportional to the square root of time as predicted theoretically by Scriven. For these bubbles the calculated supersaturation of hydrogen in the solution was found to be from eight to twenty-four times the concentration at saturation.

Little is known about bubble growth during electrolysis. Presumably the bubbles form where they do because something is special at the bubble-producing sites. The bubbles grow as fast as they can, as dictated by the conditions in the surrounding liquid. Coehn and Neumann (2) photographed a 2 cm. wide field of view on an electrode at intervals of about 3 min. and obtained breakoff diameters for many bubbles. However bubble growth rates could not be determined from their pictures. Kabanow and Frumkin (4) grew bubbles very slowly (1 to 15 hr per bubble) and also reported breakoff diameters.

Bubble growth during electrolysis is analogous to bubble growth in boiling liquids. Scriven (8) has derived equations for both cases. The object of the present investigation was to obtain data to test the expression for diffusion-controlled, isothermal bubble growth. The results constitute the only known experimental study of rapid, microscopic, bubble growth during electrolysis.

THEORY

Scriven (8) has presented a consolidated mathematical statement for the problem of spherical phase growth in an infinite medium. He gives the general case and also the simplified special cases in which growth is controlled by the transport of heat only or matter only.

For the general case the pertinent equations include a force balance, a heat balance, and a mass balance. The first of these, the equation of motion, is Equation (1) and includes forces due to pressure, surface tension, viscosity, and inertia:

$$\frac{p_v + p_i - p_\infty}{\epsilon \rho_L} = \frac{2\sigma}{\epsilon \rho_L R} + R\frac{\partial^2 R}{\partial \theta^2} + \frac{3}{2}\left(\frac{\partial R}{\partial \theta}\right)^2 + \frac{4\mu}{R}\frac{\partial R}{\partial \theta} \tag{1}$$

Equation (2) is the heat balance, with the assumption that heat transfer is by conduction only:

$$\frac{\partial T}{\partial \theta} + u\frac{\partial T}{\partial r} = \left(\frac{k_L}{\rho_L c_L}\right)\left(\frac{\partial^2 T}{\partial r^2} + \frac{2}{r}\frac{\partial T}{\partial r}\right) + \frac{Q_o}{\rho_L c_L} \tag{2}$$

Equation (3) is the mass balance, with the assumption that mass transfer is by diffusion only:

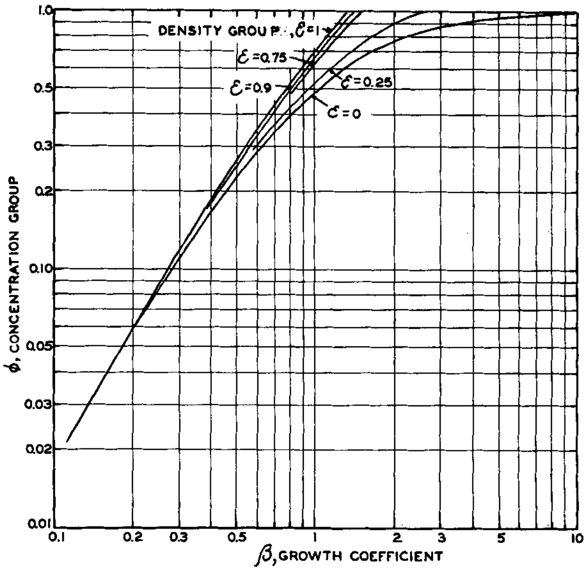

Fig. 1. Graph of Equation (5) giving the coefficient in the growth equation $R = 2\,\beta\,\sqrt{D\,\theta}$.

D. E. Westerheide is at Iowa State University, Ames, Iowa.

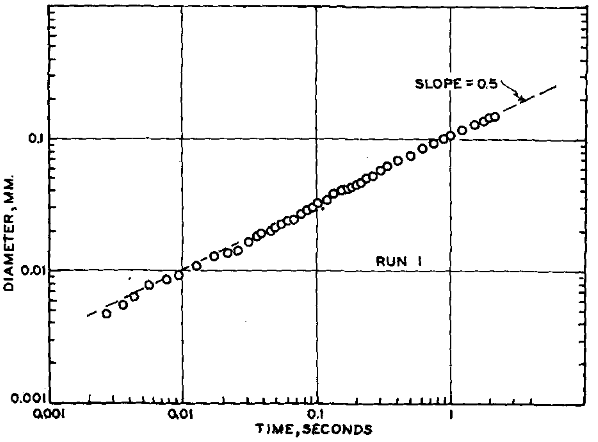

Fig. 2. Growth of a single hydrogen bubble, Run 1.

$$\frac{\partial C}{\partial \theta} + u\frac{\partial C}{\partial r} = D\left(\frac{\partial^2 C}{\partial r^2} + \frac{2}{r}\frac{\partial C}{\partial r}\right) \quad (3)$$

These three equations require spherical symmetry, an infinite body of the ambient phase, incompressible fluids, Newtonian fluids, no external body forces, no heat generation from viscosity, and the existence of not more than two components.

A rigorous simultaneous solution of the three equations is not yet practical. Thus assumptions are made which simplify the mathematics enormously. As examples surface tension is taken as negligible, and acceleration is assumed nil. The first assumption should be good except for very small bubbles. The second assumption should be good unless the phase growth is very rapid. Arguments are given for letting viscosity and p_V be zero. The results give zero for every term in Equation (1), and the equation of motion vanishes. Thus the growth of a bubble is assumed not to be limited by a balance of mechanical forces.

For the special case of isothermal bubble growth only Equation (3) is retained. It states that the rate of growth of a bubble is limited by the rate of diffusion of the dissolved solute through the liquid phase. The liquid solvent is considered nonvolatile. The detailed mathematics will not be repeated here, but the most important boundary conditions are displayed below.

At time zero, $\frac{dR}{d\theta} = 0$

At time zero, $C = C_\infty$ for all values of r

At all values of θ, $C = C_\infty$ at $r \to \infty$

At time zero the bubble is imagined to have a finite size (larger than a bubble nucleus) and to have zero radial velocity. There is no evidence that these two conditions can be met simultaneously, but the conditions are convenient for mathematical reasons.

Even with the simple model the solution of Equation (3) is difficult. Scriven assumed that the correct form of the solution is

$$R = 2\beta\sqrt{D\theta} \quad (4)$$

and showed that the coefficient β then is a function of the density and composition of each phase:

$$\phi = 2\beta^3 \exp\left(\beta^2 + 2\epsilon\beta^2\right) \int_\beta^\infty x^{-2} \exp\left(-x^2 - 2\epsilon\beta^3 x^{-1}\right) dx \quad (5)$$

where

$$\phi = \left(\frac{\rho_L}{\rho_G}\right)\left(\frac{C_\infty - C_{sat}}{\rho_L - C_{sat}}\right) \quad (6)$$

and

$$\epsilon = \frac{\rho_L - \rho_G}{\rho_L} \quad (7)$$

Scriven used a digital computer to evaluate β for various conditions. Figure 1 is a graph of Equation (5) and shows how β depends on the two dimensionless groups ϕ and ϵ. So as to indicate the region of interest for the present study the range of β has been extended 1 cycle below the range originally illustrated by Scriven.

APPARATUS

Because this study was concerned with microscopic details it was desirable to restrict the area of possible bubble growth so as to prevent hydrogen from forming outside the field of view of the microscope. Small dimensions for the cathode were also favored by a desire to form single bubbles. These factors led to the design of a microelectrode.

The microelectrode consisted of the circular tip of a 0.005-in. diameter platinum wire. The wire was surrounded by pyrex capillary tubing, leaving only the tip exposed, and was sealed in with cement. The end of the tip was ground and polished after manufacture.

The glass tube was ell-shaped and had one arm horizontal; this arm could be rotated about its geometric axis so as to orient the electrode tip either in the horizontal plane or the vertical plane. Rotation of the glass holder by 90 deg. shifted from one setup to the other.

Polishing of the cathode tip was carried out with five grades of emery cloth, the last being 4/0. The last stage used a power driven rotary disk covered with 8-oz. canvas and wetted with aluminum oxide which was fine enough to remain suspended in water for 15 min. Between stages the cathode tip was rinsed with alcohol, dried, and rotated 90 deg.

The anode consisted of a 1½-in. diameter ring of 0.025-in. platinum wire connected directly to the microscope barrel. Care was taken to insulate the supports where contact with the microscope was made. The anode was mounted in this manner because it was desired that the electrodes be the same distance apart in every experimental run. This was automatically accomplished when the microscope was focused on the cathode.

The cathode was mounted permanently in a plastic test cell. During operation the test liquid in the cell amounted to about 60 cc. The microscope was positioned above the cell, and the anode ring was in a horizontal plane for all runs.

The test liquids were 0.1 normal and 1.0 normal sulfuric acid in water. Current densities between 0.1 and 0.2 amp./sq. cm. were obtained by the use of 1.5- and 3.0-v. dry cells as a voltage source in conjunction with suitable voltage divider circuits. Currents and voltages were recorded by means of a microammeter and a potentiometer. The voltage applied to the test cell was constant during any one run. The current density was found to vary during a run, depending on the number and sizes of the bubbles on the cathode.

TABLE 1. SUMMARY OF TEST CONDITIONS

Run	Acid normality	Cathode, amp./sq. cm. Start	End	View	Number of bubbles measured	Number of bubbles on film
1	1.0	0.11	0.06	Profile	1	1
2	0.1	0.11	0.03	Profile	1	2
3	0.1	0.17	0.08	Profile	2	46
4	0.1	0.11	0.03	Plan	3	3
5	1.0	0.13	0.04	Profile	26	26
6	1.0	0.12	0.04	Plan	9	18
7	0.1	0.21	0.12	Plan	8	12

OPTICS

Illumination was provided by an arc lamp with ¼-in. diameter carbons. It was run at 4.5 amp. while the profile view was photographed and at 20 amp. while the plan view was photographed. The light beam left the lamp housing, passed through a condenser, and then was passed through a water cell to filter out the infra red.

The light beam then had either of two paths depending on whether a plan or profile view was desired. For the first case the light beam entered a vertical illuminator installed on a microscope. The light beam was reflected 90 deg. and then passed through a 10X objective, a thin cap of plastic cemented to the bottom of the objective (to prevent corrosive damage to the immersed tip of the microscope), then through the test liquid, and was focused on the cathode surface. The optical axis was normal to the electrode surface. Reflected light came back to the microscope, passed through the microscope barrel, and was brought out through a light shield to a high-speed camera. The light shield was a 14 in. length of black cardboard tubing about 2 in. in diameter.

When it was desired to photograph the electrode surface with a profile orientation, the light beam was reflected upward at the concave side of a substage mirror located beneath the test cell. In this case the electrode surface was vertical, and the light beam was also vertical as it illuminated the bubble.

With the light shield removed temporarily and a 15X eyepiece inserted in the microscope, an observer could select the desired field of view by means of two micrometer adjustments on the microscope stage which supported the test cell.

After a view was selected, the eyepiece was removed and the light shield was installed between the microscope and the camera. The camera was loaded with 16-mm, Tri-X, high-speed motion picture film. A hole was punched in the film so that final focusing could be achieved while the film was in the camera. With everything adjudged to be working properly the film was exposed.

The enlargement could be controlled by moving the camera closer to or away from the microscope and by adjustments in the objective-to-object distance. The magnifications were calibrated by photographing a stage micrometer. The image on the negative was 30.4 times the diameter of the actual bubble for the runs reported herein.

At the high magnifications used in this study vibration was a severe problem. It was finally minimized when the lamp, microscope, camera, and test cell were all mounted on a single, 6-ft., vertical, optical bench. The weight of the bench was supported by legs made of pipe which extended to floor flanges on the concrete floor. The bench was stabilized in a vertical position by securing it to a structural column with tie rods. Combinations of soft rubber and hair felt, placed at the points of contact of the bench with the floor and column, helped to eliminate the transmittance of building vibrations to the bench.

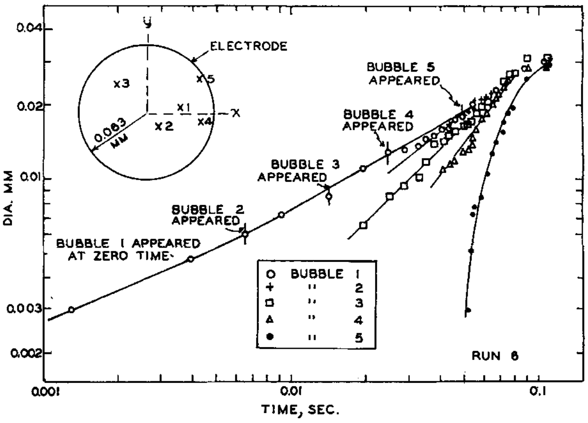

Fig. 4. Simultaneous growth of five noncoalescing bubbles, Run 6, bubble 1 originates at zero time. Sketch shows location of bubble sites on electrode.

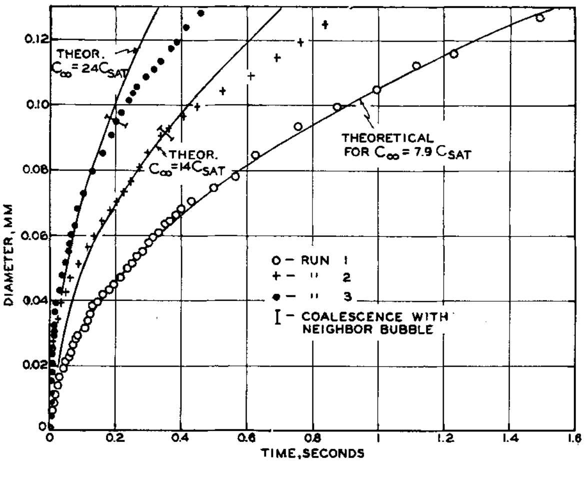

Fig. 3. Comparisons of two current densities and two normalities, Runs 1, 2, and 3.

RESULTS

The final data for this paper were obtained from seven reels of motion picture film. The conditions are recorded in Table 1. Plan views and profile views both were included, the pH was at two levels, and the current density was at two levels. The pressure was atmospheric. Diameter vs. time measurements for fifty bubbles were obtained by examining the film on a professional film editing machine. A selection of the motion picture is available on request (9).

The bubbles were all segments of spheres. The contact angle as determined from enlarged photographs was between 5 and 15 deg.

Single Bubbles

During Run 1 a single bubble was on the film for 2,835 frames. The growth of this bubble is illustrated in Figure 2. The radius is proportional to the square root of time as predicted by Scriven's equation. The data are repeated in Figure 3 with arithmetic coordinates. The close agreement with theory is somewhat surprising because true radial symmetry cannot exist during electrolysis.

For all other runs two or more bubbles were recorded on a single reel of film. For Run 2 two bubbles were seen; one started first and was several orders of magnitude larger than the second when coalescence occurred. The growth of the first bubble before and after coalescence is depicted in Figure 3. The growth before and after coalescence with a tiny neighbor of the first bubble of Run 3 also is depicted. Subsequently forty-four other bubbles appeared during this run. The theoretical parabolas are a fair fit for the first bubbles of Runs 2 and 3 and excellent for Run 1.

Figure 3 shows the effect of current density and acid normality. Runs 2 and 3 had identical conditions except that the current density was large for Run 3 and small for Run 2. As expected

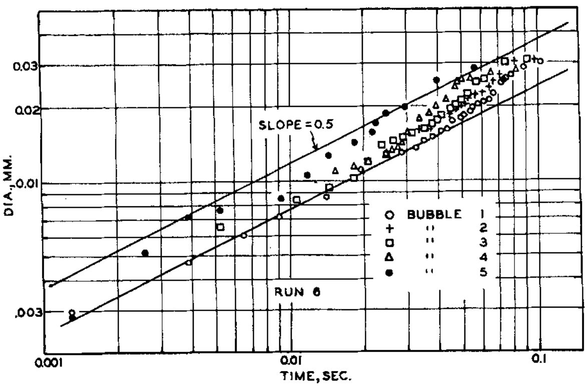

Fig. 5. Data of Figure 4 adjusted so each bubble starts at zero time.

Table 2. Location of Bubble Origins

		Coordinates in mm. x	y
Run 4	Bubble 1	−0.028	+0.038
	Bubble 2	+0.056	−0.027
Run 6	Bubble 1	+0.030	+0.007
	Bubble 2	+0.003	−0.010
	Bubble 3	−0.024	+0.022
	Bubble 4	+0.052	−0.012
	Bubble 5	+0.045	+0.037
Run 7	Bubble 1	+0.025	+0.030
	Bubble 2	+0.005	+0.012
	Bubbles 3 to 8	−0.025	+0.024

the faster growth occurred with the greater current density. Runs 1 and 2 were under identical conditions except that the acid normality was high for Run 1 and low for Run 2. The faster growth occurred with the low normality. Kraus (5) states that the equivalent conductance decreases with increasing sulfuric acid concentration. However there is doubt that the dependence of mobility of the hydrogen ions on acid concentration is sufficient to explain the bubble-growth results.

The data in Figure 3 may be used to calculate the growth constant β for each of the three runs. From β one can use Figure 1 to get ϕ and the corresponding concentration driving force. This procedure was used, with a constant diffusivity of 6.65×10^{-5} sq. cm./sec. and a solubility at saturation of 1.54×10^{-6} g./cc. assumed. These values are correct (3, 6) for hydrogen in pure water at the temperature employed, 77°F. These results indicate that the supersaturation varied from about eight to twenty-four times the saturation concentration.

Noncoalescing Multiple Bubbles

Figure 4 shows the history of the first five bubbles appearing in Run 6. The location of the bubble origins is indicated in the sketch of the electrode tip which is included in the figure. Time zero is measured from the first appearance of bubble 1. No coalescence occurred during the time indicated in Figure 4. At 0.107 sec. the first coalescence began, and others took place thereafter.

Figure 4 seems to indicate that the growth rates of the bubbles varied enormously, with the first bubble being slow and the others rapid. But this conclusion is misleading as shown in Figure 5. The same data are used, but each bubble has been adjusted to its own time zero. It is evident that the radii of all the bubbles are more or less proportional to the square root of time. The spread in the computed value of the coefficient β is about ± 25%.

Coalescing Bubbles

During Run 7 eight bubbles appeared in succession. Bubble 1 appeared first. After 0.00807 sec. bubble 2 appeared at a center-to-center distance of 0.027 mm. from bubble 1. At 0.0226 sec. the two merged to form a larger bubble which will be called *bubble 1* because 67% of its volume came from the first bubble. At 0.0836 sec. bubble 3 appeared and merged with bubble 1 at 0.1032 sec. At this time the ratio of the two bubble volumes was 23 to 1. Other bubbles appeared at the site of bubble 3, and successive coalescences took place as indicated in Figure 6. The sketch of the electrode in Figure 6 shows the location of the bubble origins. Exact locations are listed in Table 2.

The growth of bubble 1 through the course of Figure 6 is composed of two contributions. One is the normal growth by dissolution of dissolved hydrogen molecules at the bubble wall, and the other is growth by acquisition or coalescence.

This two-mode growth phenomenon occurred in Run 4 also and is depicted in Figure 7. Here an attempt is made to evaluate growth by the normal mode only. Three different time scales are used for Run 4. Bubbles 1 and 2 are assigned separate zero times corresponding to their first appearances. Bubble 3 resulted from coalescence of bubbles 1 and 2 while they were comparable in size, it was assigned a special zero time selected to force it to agree with $R = \text{const } x\,\theta^n$. This time origin is 0.053 sec. before the merger of bubbles 1 and 2, the resulting value of n is 0.29. Thus if bubble 3 had started with size zero at this computed time zero and had grown according to the 0.29 power of time, it would have the correct observed diameter at a time corresponding to the actual birth of bubble 3 from coalescence.

The exponent 0.29 is considerably less than the theoretical value of 0.5. However bubble 2 grew at a slow rate and so did bubble 1 at first. Bubble 1 eventually grew faster, but this resulted from a merger with a small unmeasured neighbor. The time scale for bubble 1 in Figure 7 was not changed after this first merger, so the apparent change in slope should be ignored. However for bubble 3 or any bubble formed by coalescence of two bubbles of comparable size there is no reason to expect agreement with theory. When coalescence takes place, the concentration field

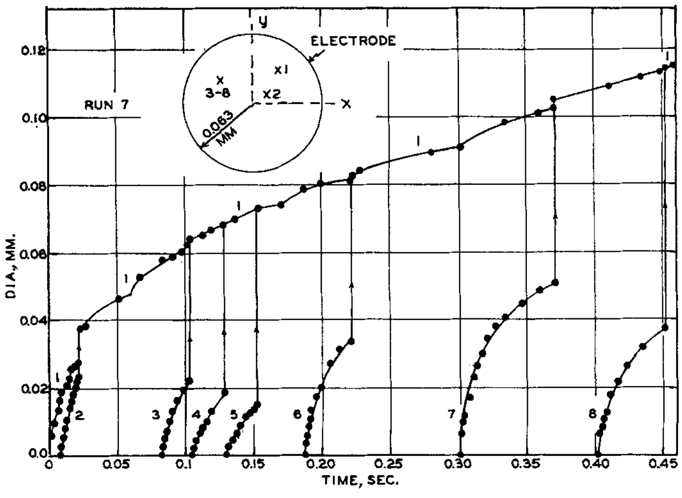

Fig. 6. Eight consecutive coalescing bubbles, Run 7. Sketch shows location of bubble sites on electrode.

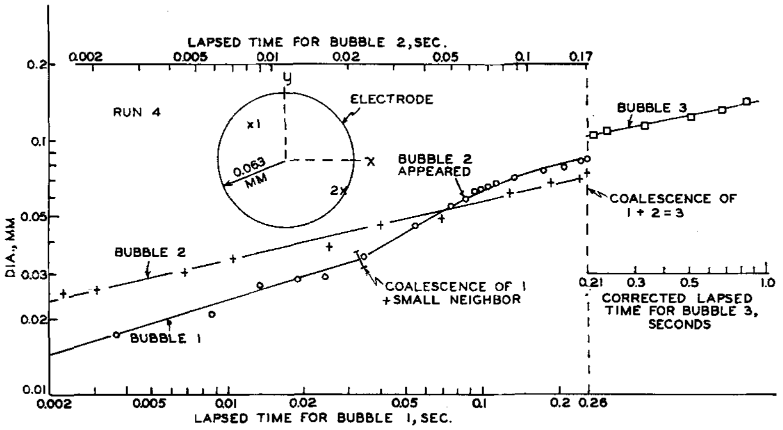

Fig. 7. Special time scales for coalescing bubbles, Run 4. Sketch shows location of bubble sites on electrode.

around two bubbles must be disturbed by the motion. The action is very rapid. An estimate from the motion pictures is that the required time for coalescence is about 3 x 10^{-4} sec. when both bubbles are roughly 0.05 mm. in diameter.

The volume of a bubble newly formed by coalescence is exactly equal to the sum of the volumes of the two previous bubbles, as expected. The center of the new bubble is exactly at the location predicted from the diameters and center locations for the two prior bubbles. Thus it is clear that both prior bubbles move toward one another during the actual coalescence, with the amount of movement of each being determined by their relative sizes. Thus coalescence results in a predictable shift in the centers of gravity of the two prior bubbles to the new center of gravity of the coalesed bubble.

Bubble Interference

The theoretical equation for bubble growth is derived for a single bubble. If a second bubble is growing nearby, how will it affect the growth of the first? The data show that in numerous cases there is a definite effect, but that as yet it is not predictable. For the single bubble of Figure 2 the curve is quite smooth. However for each of the five coexisting bubbles in Figure 5 the best fitting lines would be wavy curves not straight lines. The waviness is too pronounced to be designated as data scatter. The bubble diameters are known to within about 0.002 mm. and times are known to within about 0.0005 sec. A glance at Figure 4 shows that the slope for bubble 1 changes when bubble 2 appears. If a curve is passed through each point for bubble 3, a definite jump will appear at the time bubble 4 achieves a significant size. A line through each point for bubble 4 changes slope in a noticeable way when bubble 5 enters the scene.

In Figure 6 the curve for bubble 1 shows three discontinuities in slope in addition to the changes which must occur during the act of coalescence. As bubble 3 starts to grow, the rate of growth of bubble 1 actually increases. Similar increases occur as bubbles 6 and 7 start to grow. A reason for the speedup may be guessed. As bubble 3 expands, the surrounding liquid is pushed back. If liquid of high hydrogen concentration is pushed close to bubble 1, bubble 1 will grow faster than before.

Figure 9 shows that a speedup, apparently of this type, occurred during Run 5. Bubble 1 appeared first; when bubble 3 appeared nearby, the growth rate for bubble 1 increased.

One can argue that when two bubbles grow on the electrode they compete for the dissolved hydrogen. The result might then be a slowdown for both bubbles. Perhaps this is the explanation for the small slopes (0.23 and 0.31) observed for the first two bubbles in Figure 7. These two bubbles were rather far apart at the start (0.11 mm.), in contrast to the smaller distances encountered for the speedup instances discussed above. Perhaps the shoving of fresh solution from one bubble to another is effective only over short distances and only during the early, high-velocity period of growth.

Bubble Jump-Off

A very interesting phenomenon takes place when two bubbles of about the same size coalesce. The new bubble may jump completely off the surface and then return. The occurrence is shown in Figure 8. Figure 9 depicts bubble growth leading up to the jump-off. When two bubbles merge suddenly, the center of gravity of the new bubble will at first be on a line passing through the centers of the two parent bubbles. However the new center is too close to the solid to allow the new bubble to be a sphere with the required contact angle. Thus the bubble is in compression. Expansion causes the bubble to acquire momentum, or rather the surrounding liquid moves in with enough momentum and tears the bubble off the surface.

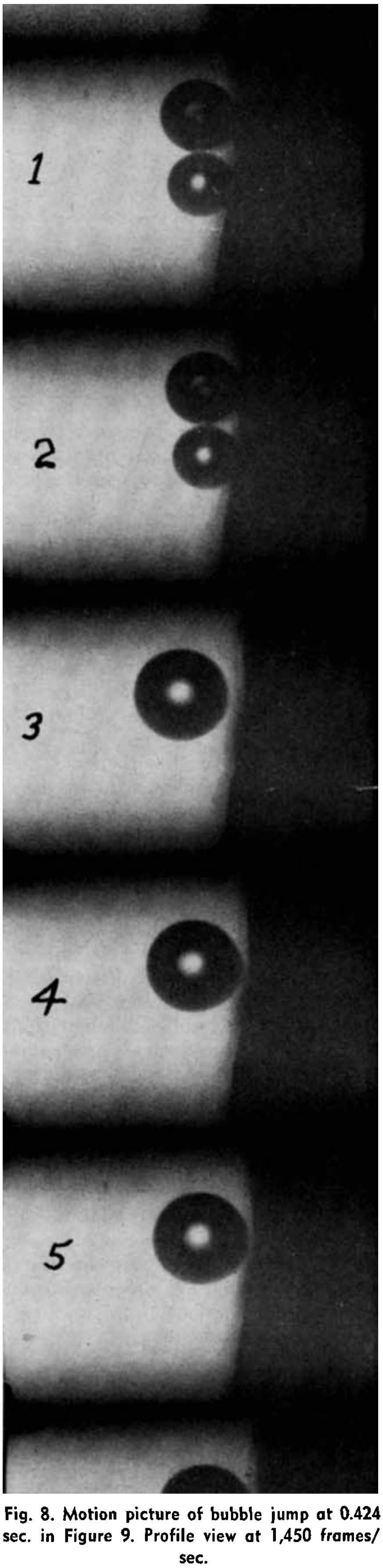

Fig. 8. Motion picture of bubble jump at 0.424 sec. in Figure 9. Profile view at 1,450 frames/sec.

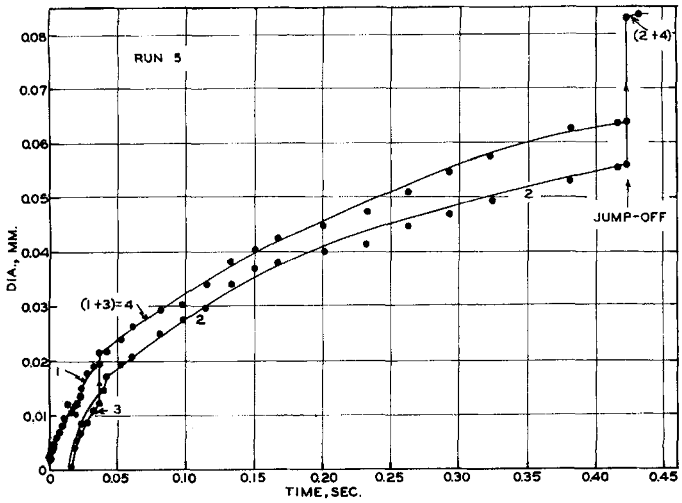

Fig. 9. Typical conditions for bubble jump, Run 5.

The maximum clear distance between a bubble and the electrode surface was 0.017 mm. This distance was reached during one frame, 0.6 x 10^{-3} sec., corresponding to an average velocity of about 3 cm./sec. and an average Reynolds number of about 4. The maximum time for the jumped bubbles to return to the surface was about 3 frames or 1.8 x 10^{-3} sec.

When two bubbles of very unequal size or two very small bubbles merge, no jump-off can be seen. When the sizes are greatly different, the large bubble seems to swallow the small one with no noticeable change in position.

After a bubble has bounced off the surface, it returns to the solid and continues to grow. Inasmuch as dissolved hydrogen is in the surrounding liquid, the bubble need not reattach to an old nucleation site to be capable of growth. The reason for the return of the bubbles is not known. It may be electrostatic attraction, on the assumption that there is a charge on a bubble different from the charge on the electrode. Kabanow and Frumkin (*4*) show that nongrowing bubbles on an electrode have no electrostatic attraction or repulsion with the electrode, but they point out that the result may be quite different for the dynamic case. A second possible reason for the bubble return is surface tension. The liquid near the electrode probably is not of uniform concentration. If surface tension is dependent on concentration, surface tension forces could cause movement.

Nucleation Sites

It is well established that during nucleate boiling bubbles form at specific nucleation sites (*1*) which exist also during electrolysis. Murakawa (*7*) states that gas bubbles of oxygen and hydrogen form at scratches on platinum. Scratches and pits were active sites during the present study. During Run 7 six consecutive bubbles formed at one site. During Run 3 forty-five consecutive bubbles were emitted at one site. Consecutive emission was observed visually (but not photographed) on many occasions. The dimensions of the sites have not been determined. Visually it is obvious that they are smaller than the sites for boiling by at least an order of magnitude.

Drift

When a bubble forms at a nucleation site, does it remain attached at that site during its entire period of on-the-solid growth? Or does the bubble slide on the surface while growing? These questions are crucial to the development of any theory of bubble mechanics, and the photographs provide the answers.

The bubbles slide during growth. The area of contact for a growing bubble increases as the bubble grows. The contact angle shows small deviations during growth, but the net change in angle is nil. It is definitely wrong to consider a bubble growing at a nucleation site similar to a rubber balloon attached to a nozzle. The bubble obtains its gas from the surrounding liquid, not from the nucleation site.

Not only does the bubble base expand during growth, but the entire bubble can slip sideways on the solid during growth. The slip was detected from motion pictures of the plan view and also the profile view. Consider Run 4. The center of bubble 1 drifted 0.007 mm as the bubble diameter increased from 0.066 to 0.085 mm. Bubble 2 drifted also. Bubble 3 formed by coalescence and drifted 0.007 mm. as it grew from 0.106 to 0.120 mm. Numerous other observations of the slip or drift of growing bubbles were made. The drift is likely caused by slight convection currents. Forced convection should cause large slip for growing bubbles.

ACKNOWLEDGMENT

Financial support was provided by the National Science Foundation. A research assistantship was given by the University of Illinois Engineering Experiment Station. Considerable help was provided by V. F. Clements, L. V. Peterson, and Sherlock Swann.

NOTATION

C = mass concentration, ML^{-3}
C_∞ = mass concentration far away, ML^{-3}
c_L = heat capacity of liquid, $HM^{-1}T^{-1}$
D = mass diffusivity, $L^2\theta^{-1}$
k_L = thermal conductivity of liquid, $H\theta^{-1}L^{-1}T^{-1}$
n = arbitrary exponent
p_i = partial pressure of inert gas in bubble, $ML^{-1}\theta^{-2}$
p_v = partial pressure of volatiles, $ML^{-1}\theta^{-2}$
p_∞ = ambient pressure, $ML^{-1}\theta^{-2}$
Q_o = heat generation per unit volume, $HL^{-3}\theta^{-1}$
r = radial coordinate, L
R = bubble radius, L
T = temperature, T
u = radial velocity, $L\theta^{-1}$
x = dummy variable, dimensionless

Greek Letters

β = growth coefficient, dimensionless
ϵ = $1 - (\rho_G/\rho_L)$, dimensionless
θ = time, θ
μ_L = kinematic viscosity of liquid, $L^2\theta^{-1}$
ρ_G = density of gas bubble, ML^{-3}
ρ_L = density of liquid, ML^{-3}
σ = surface tension, ML^{-2}
ϕ = function defined by Equation (5), dimensionless

LITERATURE CITED

1. Clark, H. B., P. H. Strenge, and J. W. Westwater, *Chem. Eng. Progr. Symposium Ser. No.* 29, **55**, p. 103 (1959).
2. Coehn, Alred, and Hans Neumann, Z. *Physik*, **20**, 54 (1923).
3. Davidson, J. F., and E. J. Cullen, *Trans. Inst. Chem. Engrs.* (*London*), **35**, p. 51 (1957).
4. Kabanow, B., and A. Frumkin, Z. *Physik. Chem.*, **A165**, 433 (1933).
5. Kraus, C. A., "Properties of Electrically Conducting Systems," The Chemical Catalog Co., New York (1922).
6. Lange, N. A., "Handbook of Chemistry," 9 ed.,p. 1092, Handbook Publishers, Sandusky, Ohio (1956).
7. Murakawa, Takao, *J. Electrochem. Soc. Japan*, **25**, No. 3, p. E61 (1957).
8. Scriven, L. E., *Chem. Eng. Sci.*, **10**, 1 (1959).
9. Westwater, J. W., and D. E. Westerheide, Motion Picture, "Growth of Hydrogen Bubbles during Electrolysis," Univ. of Illinois, Urbana, Illinois (1960).

Manuscript received July 12, 1960; revision received December 28, 1960; paper accepted January 3, 1961. Paper presented at A.I.Ch.E. Washington meeting.